

1 Theory

1.1 Dislocation lines

Several investigations have documented that dislocations in silicon give rise to characteristic photoluminescence (PL) spectra below the band edge. First showed in [9] which labeled them D1 (0.812eV), D2 (0.875eV), D3 (0.934eV) and D4 (1.000eV). The samples were deformed at 850° C by bending, so that dislocation densities were inhomogeneous along the samples. [9] states that the intensity of these lines increases when the dislocation-rich parts of the crystal are approached. At the same time the intensity of the intrinsic characteristics decreases. The distance between D1-D4 (62 ± 3 meV) corresponds to the energy of the optical phonons in silicon [9]. [9] reports D1 and D2 are dominant in heavily deformed Si crystals, while D3 and D4 predominate in weakly deformed Si. A similar result was also reported by [16] for small angle grain boundaries using cathodoluminescence.

[20] suggest that D1-D4 are due to dislocations which have been frozen in under low-shear stress. Photoluminescence under uniaxial stress shows that D1/D2 originate in the tetragonal defect with random orientation relative to $\langle 100 \rangle$ directions. [20] conclude that D3 and D4 are closely related, whereas the independent D1/D2 centers might be deformation-produced point defects in the strain region of dislocations. New lines D5 and D6 emerge when high-temperature, low-stress deformation is followed by low-temperature, high-stress deformation. [20] propose that line D5 is due to straight dislocations and D6 is due to stacking faults. [20] also suggest that D3/D4 photoluminescence is much more characteristic of the dislocations themselves than the D1/D2 emission lines. [30] state that D5 is correlated with electron-hole recombination at localized centers on separate partial dislocations. After annealing at moderate temperatures ($T > 360^\circ\text{C}$) the new lines merge into D4 [30].

The origin of D1 and D2 is not clear. It has been argued that they originate in electronic transition at the geometrical kinks on dislocations [23], point defects [20] and impurities [13] and/or from the reaction products of dislocations [21]. On the other hand, D3 and D4 lines are generally thought to be related to electronic transition within dislocation cores [15]. In addition, it has been suggested that the D3 line most likely is a phonon-assisted replica of D4 [15].

Both [9] and [20] studied plastically deformed silicon made by the Czochralski process (Cz-Si). [27] studied dislocations in multicrystalline silicon (mc-Si) and found similar lines with the entire set of D-lines shifted with around 10meV, presumably due to a strain field. Using a laser annealing technique,

[22], to introduce dislocations on a Cz-Si wafer, confirm the band location of D1-D4 from [20] in [27]. A principal difference between dislocation D'-lines in mc-Si versus D-lines in Cz-Si is a substantial broadening (60-70meV at 77K) of the D1'/D2' lines [27].

| | | | | |
|------------|---------------|---------------|---------------|---------------|
| Cz-Si [9] | D1 0.812eV | D2 0.875eV | D3 0.934eV | D4 1.000eV |
| mc-Si [27] | D1' 0.80eV | D2' 0.89eV | D3' 0.95eV | D4' 1.00eV |

Table 1: Energy positions of dislocation D-lines in Cz-Si and D' bands in mc-Si

[27] reveal a linear dependence of the band-to-band photoluminescence intensity and minority carrier lifetime across entire multicrystalline-Si wafers. Photoluminescence mapping in [27] of the 0.78eV (0.8eV) band intensity reveal a linkage to areas of a high dislocation density. This band should also be visible in room temperature [27].

[28] later found that if the contamination level is too low, or too high (dislocation decorated by metal silicate precipitates) the defect photoluminescence band vanished in room temperature. However, a relatively low contamination level of dislocations, in the order of 10 impurity atoms per micron of the dislocation length produces distinguishable defect band luminescence [28].

Dislocation related lines (D-lines) has been observed in low temperature photoluminescence spectra from the regions which included the intragrain defects [25]. They also conclude that grain boundaries are not active recombination centers. [25] also show a TO-phonon replica of the boron bound exciton at 1.093eV. Intensity of boron bound exciton from the long lifetime regions was higher than that from the short lifetime regions. D-lines reported by [20] are in a short lifetime region. For a long lifetime region, [25] observe a peak at 1.00eV which is not the D4 line, but the zonecenter optical phonon sideband of the two-hole transition in the boron bound exciton [7]. There have been no reports on the D-line spectrum missing only the D1 line [25].

[24] study origins of the defects by low temperature photoluminescence spectroscopy, electron backscatter diffraction pattern measurement and the etch-pit observation, and conclude that defects are metal contaminated dislocation clusters which originated from small angle grain boundaries.

1.2 Impurities

Diffusion of transition metals into silicon crystals result in a variety of different electrically active levels in the forbidden bandgap.

1.2.1 Atom impurities

Early work done by [7] compare intrinsic silicon from the Czochralski process with doped silicon. [7] do extensive photoluminescence study with doping atoms As, P, Sb, Bi, B, Ga, In and Al. The high intensity transverse optical lines occur at 1.0907eV, 1.0916eV, 1.0921eV, 1.0888eV, 1.0924eV, 1.0914eV, 1.0835eV and 1.092eV respectively with the different doping atoms present. Impurities like carbon complexes with many impurities in silicon, resulting in a large variety of photoluminescence centers. Detected complexes are another C atom, one oxygen atom, one N atom, one Ga atom, the four-lithium atom complex, beryllium and numerous radiation damage centres, especially involving oxygen [6]. See appendix 2 for energies.

Copper doping of silicon crystals results in an intense emission at 1.014eV [29]. [30] study Cu doped Si and observe a shoulder on the D1 line which presumably arises from Cu precipitates at the dislocation.

[4] introduce Fe atoms into a float-zone silicon crystal and observe a spectrum of 0.735eV which relate to a complex defect containing iron.

Iron images in [17] reveal internal gettering of iron to grain boundaries and dislocated regions during ingot growth.

1.2.2 Impurities bound with doping atoms

Silicon samples containing chromium-boron pairs exhibit characteristic luminescence lines in the 0.84eV region where the intensity increased linearly with laser power [5].

[18] observe a luminescence spectra around 1.07eV in boron-doped, iron-diffused crystalline silicon and suggest the source is B-Fe pairs.

1.2.3 Interaction with dislocations

Investigation in [12] show that transition-metal contamination plays an important role in the production of D-band luminescence from silicon samples containing either epitaxial stacking faults or oxidation-induced stacking faults. [22] found that Cu doping resulted in reduced intensity of D1 and D2, and the intensity of D3 and D4 become very small. [30] demonstrate that a complete passivation of the D-band luminescence is achieved at higher

Cu and Fe concentration when deliberately contaminating high purity silicon samples which contain dislocations. However impurities like Ni, lead to no detectable changes in the spectrum [30]. D-band recombination in Si is found to be independent of impurities trapped at dislocations [30], and [21] concluded that metallic impurities don't seem to be related to D1 and D2 luminescence.

Electron hole droplets (EHD), free excitons (FE) and bound excitons (BE) localized on phosphorus atoms has been steadily observed in [8] with photoluminescence on samples with low-dislocated regions. When increasing dislocation density the FE, BE and EHD bands decrease sharply. This may be due exciton capture by dislocation lines D1,D2 and non-radiative recombination [8]. EHD photoluminescence intensity is highly dependent on the pumping power [19]. There is a linear dependence, and pumping with 3mW or less makes it hardly visible in [19].

Room temperature mapping of the 0.77eV band is attributed to oxygen precipitates in thermally treated silicon made by the Czochralski process (Cz-Si) [26]. This band peak shifts parallel to the bandgap with temperature. The increase of this band on the dislocation lines is due to the preferential precipitation of oxygen [26].

[14] state that the deep-level emission from multicrystalline silicon with an intensity maximum at 0.78eV at room temperature is different from that of the D1 line at low temperature. Furthermore, [14] suggest that the 0.78eV emission is associated with oxygen precipitation, and that the intra-grain defects are dislocation clusters decorated with oxygen impurities in addition to heavy-metal impurities. [10] state that the origin of trap densities in multicrystalline silicon could be structural crystal defects, which are highly decorated with oxygen precipitates.

References

- [1] T. Arguirov, W. Seifer, G. Jia, and M. Kittler. Photoluminescence study on defects multicrystalline silicon. *Semiconductors*, 2006.
- [2] Tz. Arguirov, W. Seifert, M. Kittler, and J. Reif. Temperature behaviour of extended defects in solar grade silicon investigated by photoluminescence and ebic. *Elsevier B.V.*, 2003.
- [3] S. Binetti, J. Libal, M. Acciarri, M. Di Sabatino, H. Nordmark, E.J. Øverlid, J.C. Walmsley, and R. Holmestad. Study of defects and impurities in multicrystalline silicon grown from metallurgical silicon feedstock. *Materials Science and Engineering B*, 2008.
- [4] M.I. C     and M.C. do Carmo. Luminescence from an iron related deep center in silicon. *Physica Scripta*, 1988.
- [5] H. Conzelmann and J. Weber. Photoluminescence from chromium-boron pairs in silicon. *Physica*, 1983.
- [6] Gordon Davies. The optical properties of luminescence centres in silicon. *Physics Report*, 1988.
- [7] P. J. Dean, J.R. Haynes, and W.F. Flood. New radiative recombination processes involving neutral donors and acceptors in silicon and germanium. *Physical Review Volume 161 Number 3*, 1967.
- [8] N. Drozdov and A. Fedotov. Electron-hole drops in dislocational silicon. *Microelectronic Engineering* 66, 2002.
- [9] N. A. Drozdov, A.A. Patrin, and V.D Tkachev. Recombination radiation on dislocations in silicon. *Pis'ma Zh. Eksp. Teor. Fiz.*, 1976.
- [10] Paul Gundel, Martin C. Shubert, and Wilhelm Warta. Origin of trapping in multicrystalline silicon. *Journal of applied physics*, 2008.
- [11] R.B. Hammond, TC. McGill, and J.W. Mayer. Temperature dependence of the electron-hole-liquid luminescence in si. *Physical Review B*, 1975.
- [12] V. Higgs, M. Goulding, and P. Kightley. Characterization of epitaxial and oxidation-induced stacking faults in silicon: The influence of transition-metal contamination. *Appl. Phys. Lett.*, 1992.
- [13] V. Higgs, P. Kightley, P.J. Goodhew, and P.D. Augustus. Metal-induced dislocation nucleation for metastable sige/si. *Appl. Phys. Lett.*, 1991.

- [14] M. Inoue, H. Sugimoto, M. Tajima, Y. Ohshita, and A. Ogura. Microscopic and spectroscopic mapping of dislocation-related photoluminescence in multicrystalline silicon wafers. *J. Mater Sci*, 2007.
- [15] V.V Kveder, E.A. Steinman, S.A. Shevchenko, and H.G. Grimmeiss. Dislocation-related electroluminescence at room temperature in plastically deformed silicon. *Phys. Rev. B*, 1995.
- [16] Woong Lee, Jun Chen, Bin Chen, Jiho Chang, and Takashi Sekiguchi. Cathodoluminescence study of dislocation-related luminescence from small-angle grain boundaries in multicrystalline silicon. *Applied Physics Letters*, 2009.
- [17] D. Macdonald, J. Tan, and T. Trupke. Imaging interstitial iron concentrations in boron-doped crystalline silicon. *Journal of applied physics*, 2008.
- [18] H.D. Mohring, J. Weber, and R. Sauer. Photoluminescence of excitons bound to an isoelectronic trap in silicon associated with boron and iron. *Physical Review B*, 1983.
- [19] Satoshi Nihonyanagi and Yoshihiko Kanemitsu. Enhanced luminescence from electron-hole droplets in silicon nanolayers. *Applied physics letters*, 2004.
- [20] R. Sauer, J. Weber, and J. Stolz. Dislocation-related photoluminescence in silicon. *Appl. Phys.*, 1985.
- [21] T. Sekiguchi and K. Sumino. Cathodoluminescence study on dislocations in silicon. *J. Appl. Phys.*, 1995.
- [22] W. Staiger, G. Pfeiffer, K. Weronek, A. Höpner, and J. Weber. Dislocation-induced defect levels in silicon. *Materials Science Forum*, 1994.
- [23] M. Suezawa, Y. Sasaki, and K. Sumino. Dependence of photoluminescence on temperature in dislocated silicon crystals. *Physica Status Solidi*, 1983.
- [24] H. Sugimoto, K. Araki, M. Tajima, T. Eguchi, I. Yamaga, M. Dhamrin, K. Kamisako, and T. Saitoh. Photoluminescence analysis of intragrain defects in multicrystalline silicon wafers for solar cells. *Journal of Applied Physics*, 2007.

- [25] Hiroki Sugimoto, Masaaki Inoue, Michio Tajima, Atsushi Ogura, and Yoshio Ohsita. Analysis of intra-grain defects in multicrystalline silicon wafers by photoluminescence mapping and spectroscopy. *Japanese Journal of Applied Physics*, 2006.
- [26] M. Tajima, M. Tokita, and M. Warashina. Photoluminescence due to oxygen precipitates distinguished from the d-lines in annealed si. *Materials Science Forum*, 1995.
- [27] I. Tarasov, S. Ostapenko, C.Haessler, and E.-U. Reisner. Spatially resolved defect diagnostics in multicrystalline silicon for solar cells. *Elsevier Science S.A*, 2000.
- [28] I. Tarasov, S. Ostapenko, W. Seifert, M. Kittler, and J.P. Kaleis. Defect diagnostics in multicrystalline silicon using scanning techniques. *Elsevier Science B.V.*, 2001.
- [29] J. Weber, H. Bauch, and R. Sauer. Optical properties of copper in silicon: Excitons bound to isoelectronic copper pairs. *Physical Review B*, 1982.
- [30] K. Weronek, J. Weber, and R. Buchner. Origin of d-band photoluminescence in silicon. *Springer Proceedings in Physics*, 1991.

A Silicon energy bands

| Energy | Name | Temp. | Impurity / Defect | Observed in |
|-------------|-----------------------------------|----------|--|---------------|
| 0.735eV | ZPL | 22K | Fe contamination | [4] |
| 0.745eV | C-N | | Carbon-Nitrogen complex | [6] |
| 0.76-0.8eV | Defect | 290K | Dislocation with low contamination | [27] [28] [1] |
| 0.77-0.78eV | D _b | 4.2-295K | Oxygen impurity band | [26] [14] |
| 0.77eV | P line | 12K | C-O complex related | [6] [3] |
| 0.780eV | CrB ^{0Γ} | 4.2K | CrB ⁰ phonon replica | [5] |
| 0.79eV | C-O | 12K | Carbon-Oxygen complex | [6] [3] |
| 0.80eV | D1' | 77K | Dislocations ¹ | [27] [28] |
| 0.812eV | D1 | 4.2K | Dislocation related line ¹ | [9] [20] [2] |
| 0.8160 | CrB ² | 4.2K | Cr-B excitation of local vibrations | [5] |
| 0.8402 | CrB ¹ | 4.2K | Cr-B excitation of local vibrations | [5] |
| 0.8432eV | CrB ⁰ | 4.2K | Cr-B pair no-phonon | [5] |
| 0.875eV | C-Ga | | Carbon-Gallium complex | [6] |
| 0.875eV | D2 | 4.2K | Dislocation related line ¹ | [9] [20] [2] |
| 0.89eV | D2' | 77K | Dislocations ¹ | [27] [28] |
| 0.8-0.9eV | D _{a1} | 11K | Broad background emission under D1/D2 | [26] |
| 0.91eV | H-line | 12K | C-O complex related | [6] [3] |
| 0.93eV | H-line | 12K | C-O complex related | [6] [3] |
| 0.934eV | D3 | 4.2K | Dislocations ² | [9] [20] [2] |
| 0.95eV | D3' | 77K | Dislocations ² | [27] [28] |
| 0.953eV | D5 | 4.2K | Straight dislocations | [20] [30] |
| 0.968eV | I ^{TO+20Γ} | 26K | TO + 2 Zone center phonon | [7] |
| 0.969eV | C-C | | Carbon-Carbon complex | [6] |
| 0.98eV | R2BB | 80K | Two phonon replica of band edge emission | [2] |
| 0.9-1.0eV | D _{a2} | 11K | Broad background emission under D3/D4 | [26] |
| 1.000eV | D4 | 4.2K | Dislocations ² | [9] [20] [2] |
| 1.00eV | D4' | 77K | Dislocations ² | [27] [28] |
| 1.0089eV | FeB ⁰ (TO) | 6K | Fe-B pair phonon replica | [18] |
| 1.0126eV | D6 | 4.2K | Stacking faults | [20] [30] |
| 1.013eV | I ^{TO+0Γ+IV^a} | 26K | TO + 0Γ + IV ^a phonon | [7] |
| 1.014eV | Cu ₀ | 4.2K | Copper doping | [29] [30] |
| 1.018eV | W/I1 | | Radiation damage | [6] |
| 1.0315eV | I ^{TO+0Γ} | 26K | TO + Zone center phonon | [7] |
| 1.04eV | R1BB | 80K | One phonon replica of band edge emission | [2] |
| 1.045eV | Q | | 4-Li atom complex | [6] |
| 1.0504eV | FeB ² | 6K | Fe-B pair contamination | [18] |
| 1.051eV | I ^{TO+IV^b} | 26K | Inter valley phonon replica | [7] |

Continued on next page

Table 2 – continued from previous page

| Energy | Name | Temp. | Impurity / Defect | Observed in |
|----------|--------------------------------|-------|--|---------------|
| 1.0595eV | FeB ¹ | 6K | Fe-B pair contamination | [18] |
| 1.0692eV | FeB ⁰ | 6K | Fe-B pair no phonon | [18] |
| 1.074eV | I ^{TO+IV^a} | 26K | Inter valley phonon replica | [7] |
| 1.078 | EHD | 4.2K | Electron Hole Droplet dislocation-area | [8] |
| 1.082eV | EHD _{TO} | 4.2K | Electron Hole Droplet dislocation-free | [11] [8] [19] |
| 1.0835eV | In ^{TO} | 30K | Indium doping TO | [7] |
| 1.0888eV | Bi ^{TO} | 15K | Bismuth doping TO | [7] |
| 1.0902eV | Al ^{TO} | 30K | Aluminum doping TO | [7] |
| 1.0907eV | As ^{TO} | 15K | Arsenic doping TO | [7] |
| 1.0907eV | Ga ^{TO} | 15K | Gallium doping TO | [7] |
| 1.0916eV | P ^{TO} | 15K | Phosphorus doping TO | [7] |
| 1.092eV | BE1 | 4.2K | Bound exciton | [9] |
| 1.0921eV | Sb ^{TO} | 15K | Antimony doping TO | [7] |
| 1.0970eV | I ^{TO} /FE | 26K | Transversal Optical/Free exciton | [7] [11] [8] |
| 1.0924eV | B ^{TO} | 15K | Boron doping TO | [7] |
| 1.093eV | B _{TO} | 4.2K | TO phonon replica of Boron bound exciton | [24] [14] |
| 1.1365eV | I ^{TA} /LO/FE | 26K | Transversal Acoustic/Longitudinal/FE | [11] [7] |
| 1.1545eV | I ⁰ | 26K | No phonon | [7] |

Table 2: Silicon energy bands

¹D1 and D2: It has been argued that they originate in electronic transition at the geometrical kinks on dislocations [23], point defects [20] and impurities [13] and/or from the reaction products of dislocations [21].

²D3 and D4 lines is generally thought to be related to electronic transition within dislocation cores [15]. In addition, it has been suggested that the D3 line most likely is a phonon-assisted replica of D4 [15].

B Sample types and procedures

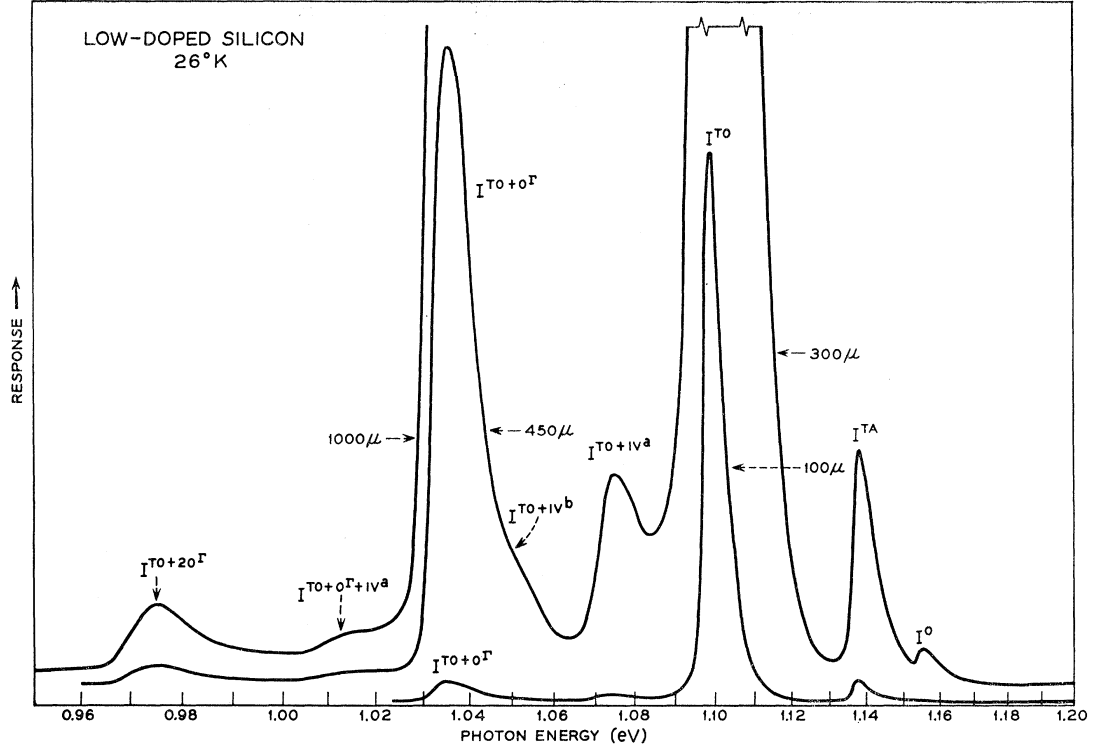


Figure 1: Low doped ($2 \cdot 10^{14} cm^{-3}$ P atoms) n-type Si PL specter from [7]

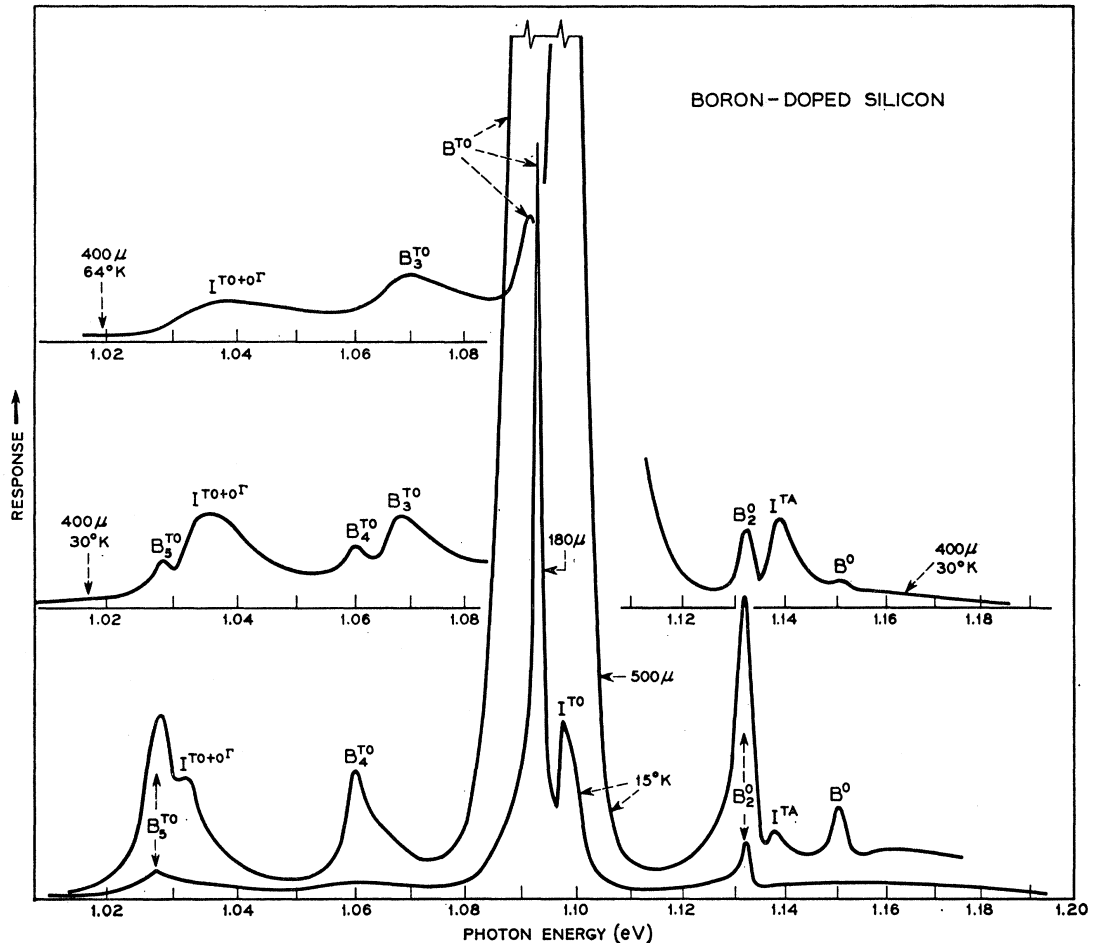


Figure 2: Boron doped ($6 \cdot 10^{16} \text{cm}^{-3}$) Si PL specter from [7]

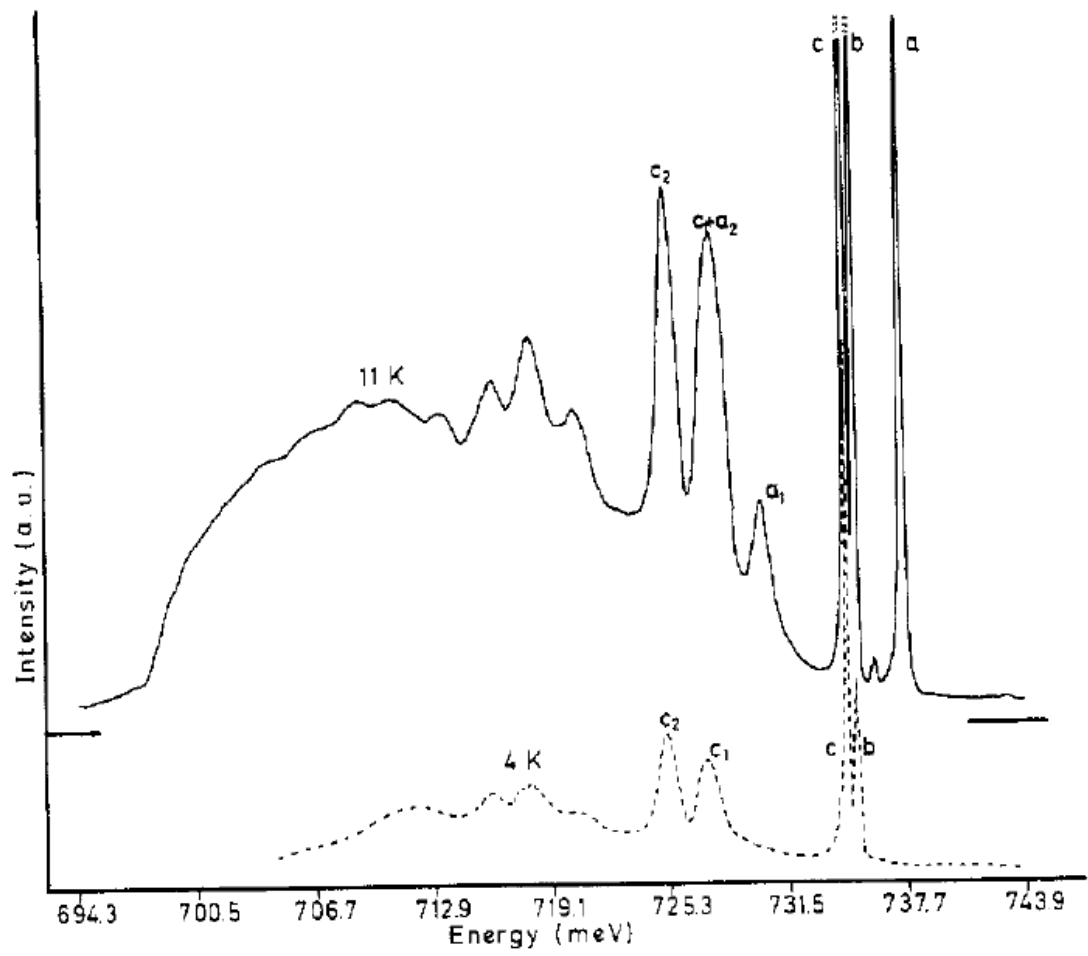


Figure 3: Iron diffused Si sample at two different temperatures from [4]

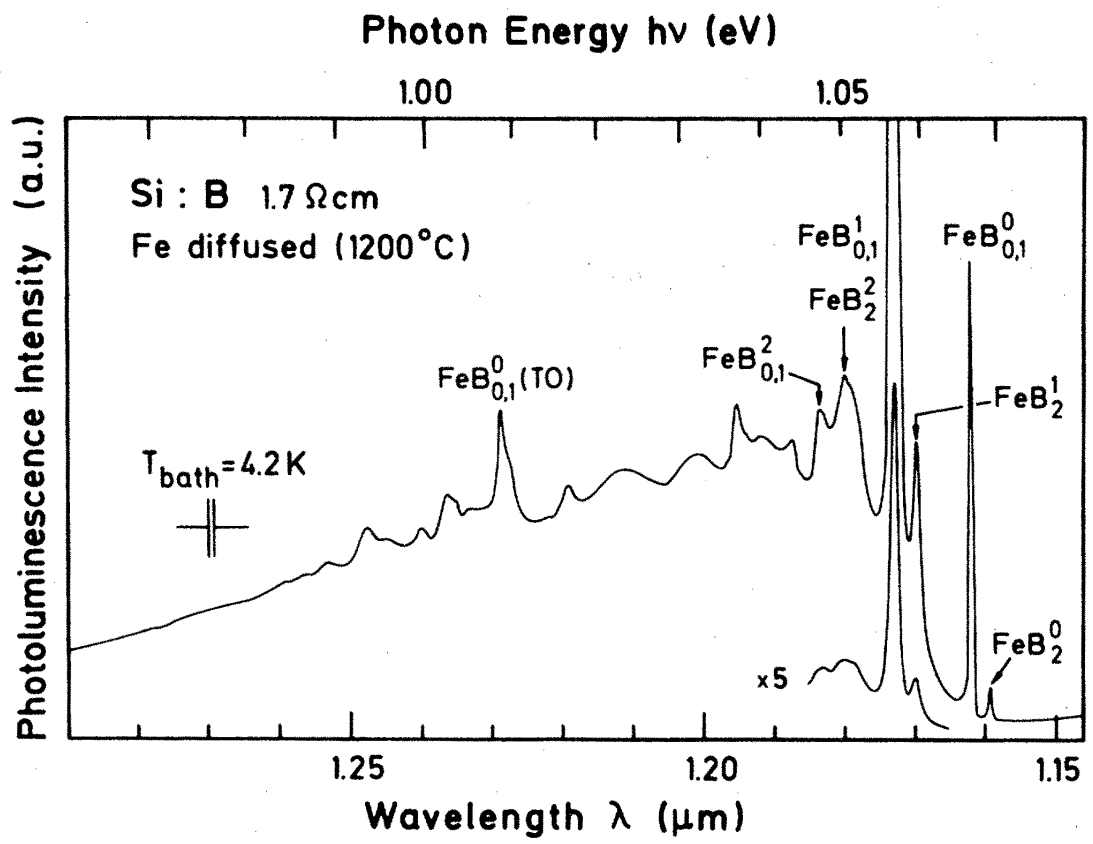


Figure 4: Iron diffused boron doped Si sample from [18]

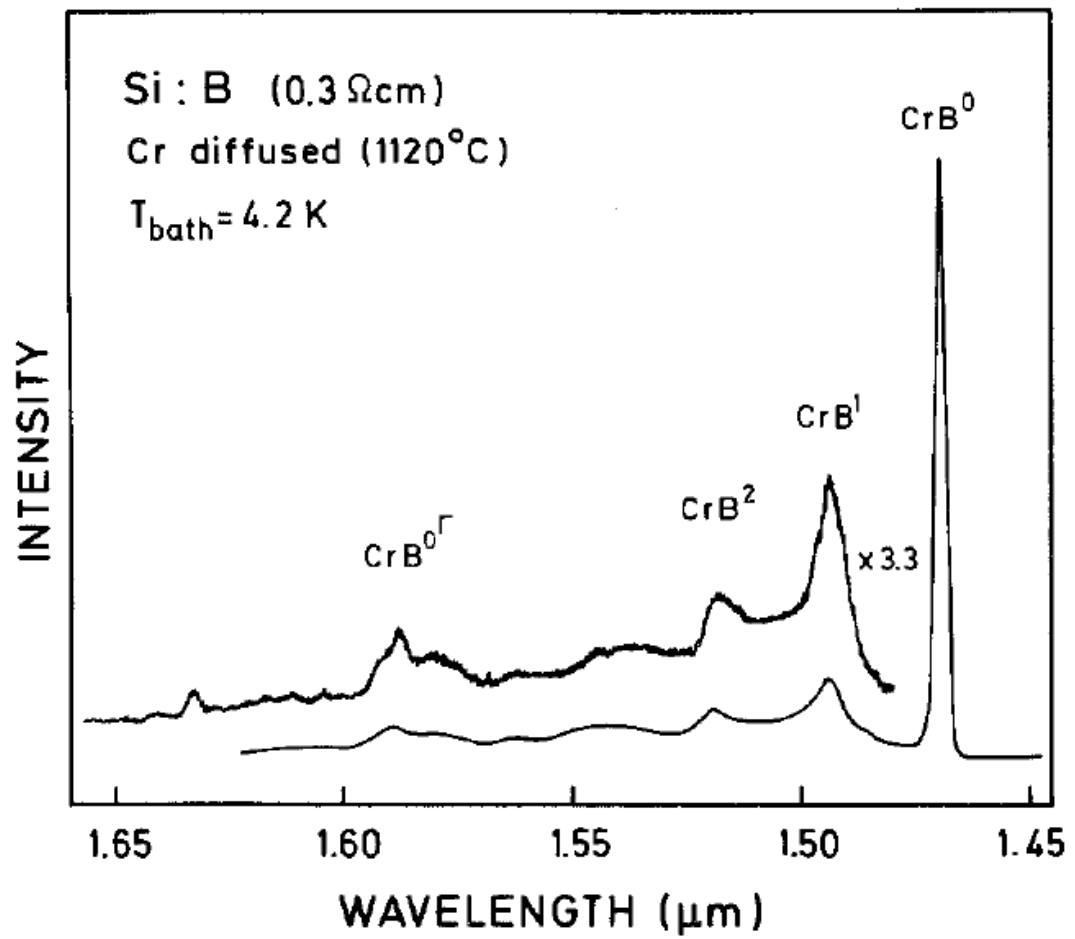


Figure 5: Chromium diffused Boron doped Si sample from [5]

| Ref. | Sample type | Excitation process | Area | Processing | Doping |
|------|-----------------|---|------------------------------|---|------------------------------------|
| [24] | mc-Si | 532nm Nd:YVO ₄ | 0.1mW/10 μ m diameter | Sawing damage etched by HNO ₃ /HF | B-doped |
| [26] | Cz-Si | Kr ion laser 647nm | 10 μ m | | Undoped |
| [9] | Cz-Si | Xenon lamp | 50mW on 3mm modulated at 9Hz | deformed by bending at 850° C | undoped, weak n and p |
| [27] | mc-Si | 800nm AlGaAs laser | Pulsed 300mW / 3mm | | Block-casting technique for Baysix |
| [28] | mc-Si | 800nm AlGaAs at 140mW | | Produced by EFG | |
| [2] | mc-Si and FZ-Si | Ar ion 514nm at 300mW | 100 μ m | Produced by EFG | boron doped $10^{15}cm^{-1}$ |
| [20] | FZ-Si | Kr-ion 647nm, Ar-ion 415nm and Nd-YAG 1064nm | | Deformed a 650° C and 850° C | residual $10^{12}cm^{-3}$ boron |
| [14] | mc-Si | Nd:YVO 532nm | 6mW, 10 μ m diameter | Slicing damage etched off by HNO ₃ /HF | boron doped |
| [5] | FZ-Si and CZ-Si | | 50mW laser | Etched with HNO ₃ /HF. Chromium diffused | boron doped |
| [18] | FZ-Si | Ar+ 514nm | 500mW | Fe diffused | boron doped |
| [4] | FZ-Si | Argon laser | | Fe diffusion | undoped |
| [29] | | Ar ⁺ 514nm at 1.5W | | | Cu doped |
| [30] | FZ-Si | Ar ⁺ 514nm | | Heated above a Bunsen burner | Doped with Cu and/or Fe |
| [3] | mc-Si | | 6W/cm ² | Polished by HNO ₃ /HF | Undoped |
| [7] | CZ-Si | 200W mercury arc 2.5eV | | | Undoped and doped |
| [8] | | Ar ⁺ or Kr ⁺ laser 0.6W | 0.8mm diameter | Dislocations by bending at 700° C | phosphorus doped |

Table 3: Sample types and procedures